EXPERIMENTAL INVESTIGATION OF ULTRA-HIGH VACUUM ADHESION AS RELATED TO THE LUNAR SURFACE

THIRD QUARTERLY PROGRESS REPORT
1 JANUARY THROUGH 31 MARCH 1965

J. A. Ryan
Principal Investigator
R&D/Space Physics and
Planetary Sciences Branch

Prepared for:
NASA/Office of
Advanced Research & Technology
Washington, D. C.

Contract NAS 7-307

Date of Issue:
26 June 1964
A-260-BBK2-47

MISSILE & SPACE SYSTEMS DIVISION
DOUGLAS AIRCRAFT COMPANY, INC.
SANTA MONICA, CALIFORNIA

TABLE OF CONTENTS

1.0 INTRODUCTION

This report presents a summary of the work accomplished during the period January through March 1965 on the study of the ultra-high vacuum frictional-adhesional behavior of silicates as related to the lunar surface.

The purpose of this program and the approach used have been detailed in the previous reports. Basically, the purpose is to obtain data relating to the possible behavior of silicates at the lunar surface and to determine the degree to which this behavior can pose problems to lunar surface operations. The approach being used is to obtain quantitative data relating to silicate vacuum friction-adhesion through the use of "single crystal" samples of the various common silicate minerals, and through careful experimental controls. With this approach it is hoped that a basic understanding of the physics of silicate behavior in vacuum can be obtained, and hence that information of value to the lunar program can be provided.

The first reliable silicate adhesional data have been obtained during this quarter. They indicate a definite load dependence for the adhesion as well as a mineral dependence, and give indications, for given faces in contact, of a crystallographic orientation sensitivity. Adhesion forces in excess of 0.4 gm have been detected.

2.0 DISCUSSION

2.1 Vacuum System

In the previous quarterly report, it was noted that problems had arisen as to proper seating of the UHV valve. This problem has been eliminated

by improving the techniques used in reforming the value seat.

The high temperature sample bakeout, by means of an external (to the vacuum system) heater, has proven inadequate. This technique has caused pressure rises into the 10^{-7} - 10^{-8} mm Hg range and as such has to a significant degree negated the value of the bakeout. Because of this, an electron heating-bombardment system has been designed and will be incorporated into the system in the near future. This system is shown in Figure 1. The electron gun, enclosed in a quartz container, is mounted on a metal bellows. This bellows permits the gun to be inserted between the samples when desired and as such allows surface cleaning to be carried out without any significant shadowing of the surfaces to be cleaned. The quartz jacket prevents contamination from the emitting filament from entering the UH vacuum system. The interior of the gun will be maintained, by means of a second, mechanical, pumping system, at 10^{-3} mm Hg during gun operation.

It was concluded, during this quarter, that aligning the contacting sample faces to parallelism prior to pump-down not only involved an excessive amount of time but also invalidated the prior surface cleaning (the major problem is surface contamination from atmospheric aerosols). Hence, means have been provided for obtaining sample parallelism while the system is evacuated. The bottom sample has been mounted on a copper plate welded to a stainless steel bellows. Three micrometer screws attached to the base plate permit alteration of bottom sample orientation. This modification has proven to be highly successful.

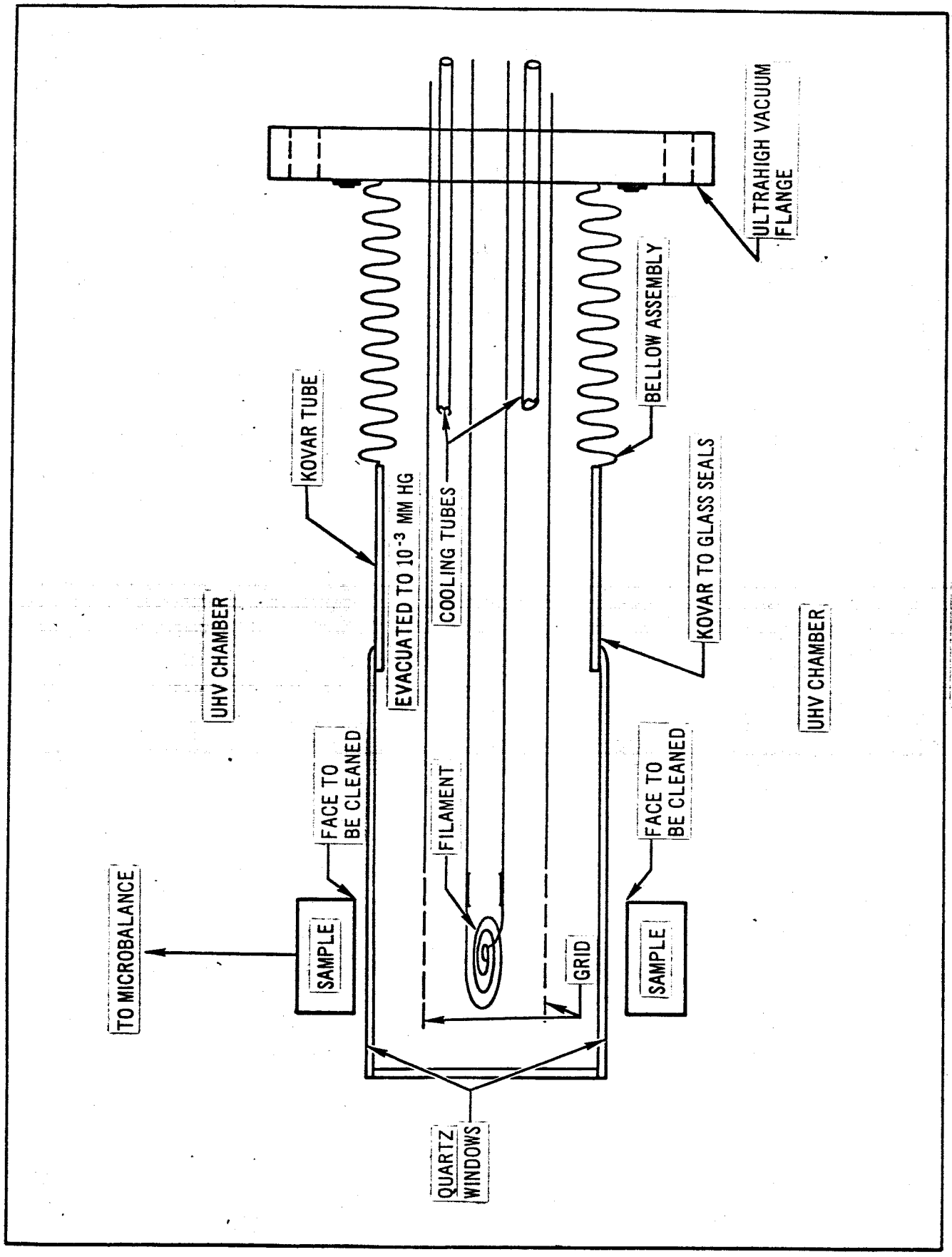
ULTRAHIGH VACUUM FLANGE
BELLOW ASSEMBLY
KOVAR TO GLASS SEALS
KOVAR TUBE
EVACUATED TO 10^{-3} MM HG
COOLING TUBES
UHV CHAMBER
UHV CHAMBER
FACE TO BE CLEANED
FACE TO BE CLEANED
FILAMENT
GRID
SAMPLE
SAMPLE
TO MICROBALANCE
QUARTZ WINDOWS
Electron Gun

Figure 1

2.2 The Microbalance

It was noted in the previous report that problems had arisen in maintaining the microbalance zero. In an effort to correct this, low melting point counterweights were used (the unbalance was in the direction of a loss of sample weight). Partial evaporation of these counterweights, to restore balance, proved to be an undesirable technique due to the excessive time involved and the unavoidable introduction of contaminents into the system. A second approach, utilizing multiple zero reference lines, was then tried. This was also found to be unsuitable since often the microbalance pointer would move to a position where precise positioning with respect to the zero lines was not possible, and hence considerable reading sensitivity was lost. It was finally decided that the only suitable approach to the problem was to provide some means of re-zeroing the balance while at vacuum. Accordingly, the experimental chamber has been modified to include a manueverable arm attached to a metal bellows with standoff, and an additional view port. With the movable arm it is now possible to adjust the coarse balance zero. The balance is then calibrated after the system is let up to dry nitrogen (instead of immediately prior to evacuation). This technique has proven to be highly successful.

2.3 Vibration Isolation System

The vibration problems encountered with the experimental system were detailed in the previous quarterly reports, along with the method devised for overcoming them. The method finally decided upon consisted of suspending the entire vacuum system from "soft" springs. The suspension system was completed during this quarter and was found to perform satisfactorily,

though it was found necessary to apply oil/vane damping to prevent excessive delays between measurements.

2.4 Experimental Data

2.4.1 Introduction

Data concerning adhesion versus load have been obtained during this quarter. Runs have been made with orthoclase (001) contacting orthoclase (001) with the respective a-b axes 80° from atomic match in orientation; orthoclase (001) contacting orthoclase (001) with the a-b axes 10° from atomic match in orientation; orthoclase (001) contacting hypersthene (110) with the a-axis of the orthoclase 45° to the c-axis of hypersthene; orthoclase (001) contacting albite (001) with the a-b axes 10° from atomic match in orientation; and orthoclase (001) contacting pure aluminum. The data show a definite load dependence for the adhesion and additional variations dependent upon the mineral used. They also indicate, for given mineral faces in contact, a dependence upon crystallographic orientation. Adhesion forces in excess of 0.4 gm have been detected with applied loads of 500 to 1000 gm, and with surface height irregularities greater than 5 microns present. Information pertaining to the nature of the adhesion forces acting has been obtained. Details of the data obtained and interpretations are given in the following sections.

2.4.2 Sample Pairs and Data Obtained

a. Orthoclase (001) vs Orthoclase (001)

Orthoclase is a member of the Feldspar Group with a composition approximately equal to $KAlSi_3O_8$. It belongs to the monoclinic crystal system and

has a Mohs hardness of 6. Orthoclase is one of the most common minerals in igneous rock, particularly the more acidic types, and is also found as a minor constituent in meteorites. The source locality for the orthoclase samples used in this study is India. The sample identity has been checked with the petrographic microscope. No twinning is present.

The orthoclase (001) plane is a "perfect" cleavage plane and represents the plane along which fracture, during comminution, occurs most readily. Two orthoclase sample pairs were fabricated. The surface roughness profiles of these samples are shown in Figures 2 through 10. These profiles have been obtained by means of a Bendix Proficorder. This instrument provides maximum sensitivity of about 700A° per division perpendicular to surface and 2.5 microns per division parallel to the surface (see the noted figures to obtain chart spacing of the divisions).

Roughness plots for the bottom sample used in the 80° orientation run are shown in Figures 2 and 3. A hump is evident in the center of the sample. The top of this hump is about 7 microns above the sample edges. Superimposed upon this is a surface roughness with an average peak to peak amplitude of about 1.5 microns, with occassional peaks projecting over 3 microns above the ground level. The cause of the hump is not known. However, a light polish was applied to the surface and though care was taken to avoid rocking of the sample, it is possible that the polishing is responsible for this effect.

Figures 4 and 5 show roughness plots of the top sample used in the 80°

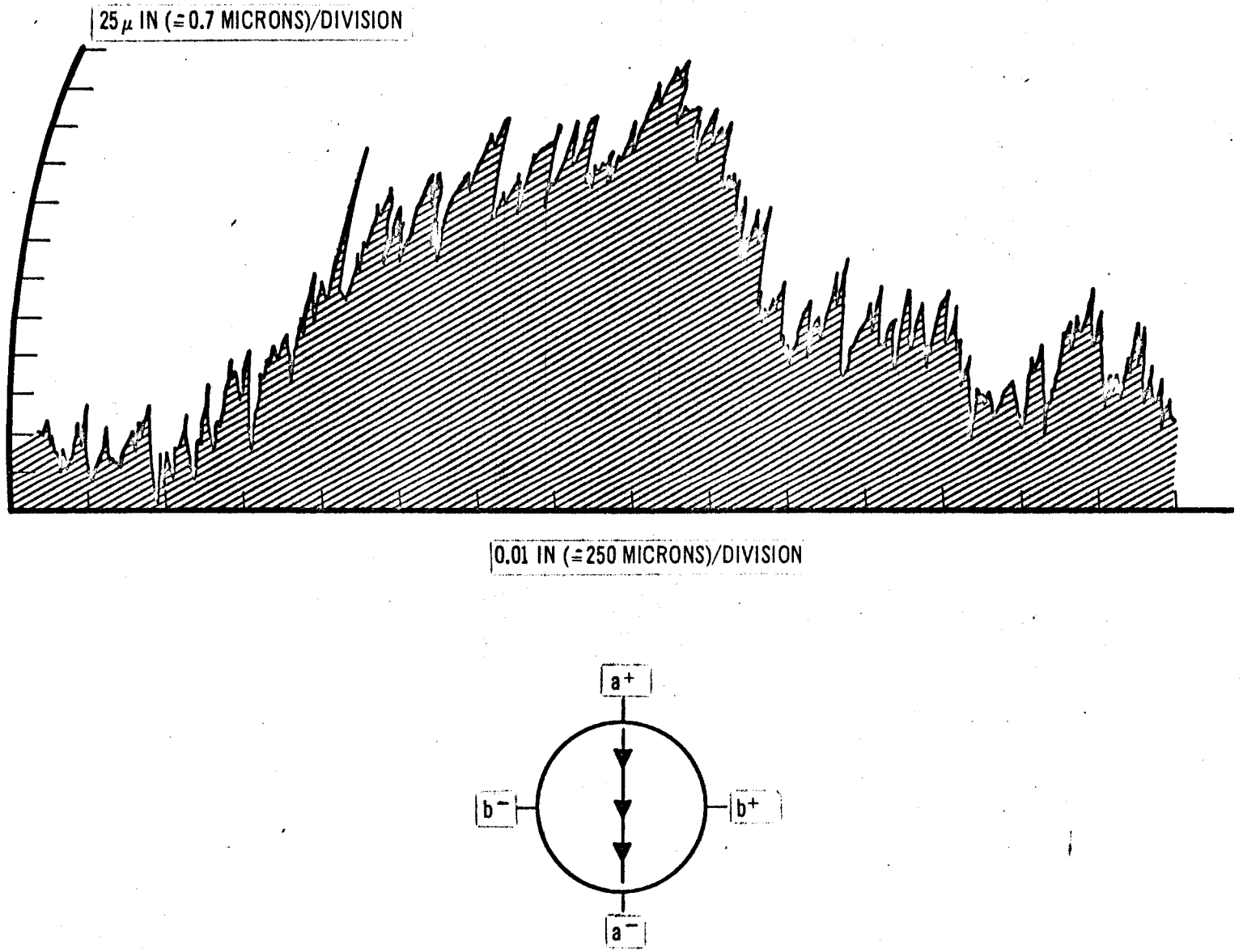

Figure 2

Run #1 Orthoclase (001)/Orthoclase (001) Bottom Sample Surface Roughness Along A-Axis

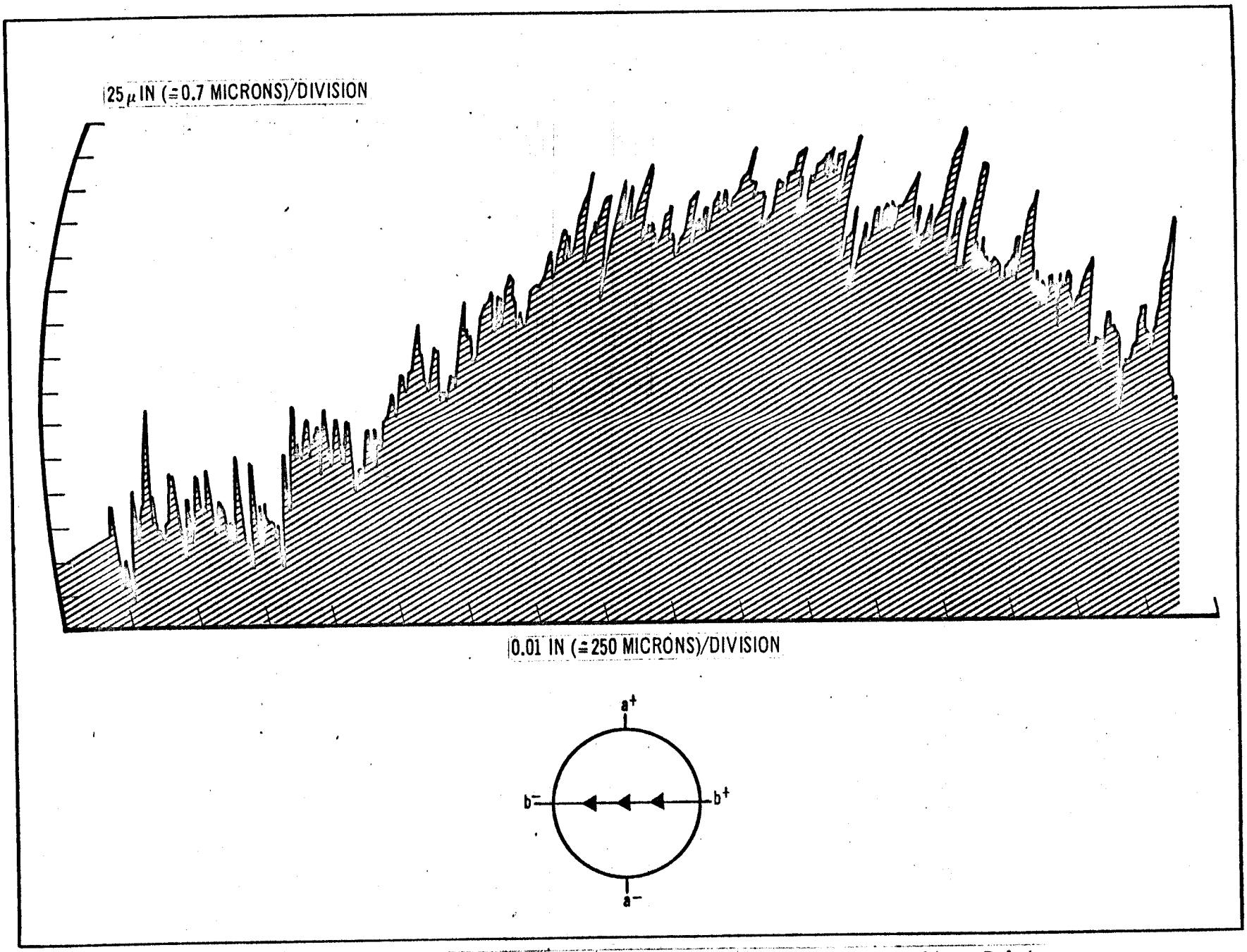

Figure 3

Run #1 Orthoclase (001)/Orthoclase (001) Bottom Sample Surface Roughness Along B-Axis

orientation run. A hump of amplitude of about 4 microns is present on the a-axis. Figure 6 shows additional traces along the a-axis (with the higher frequency surface roughness filtered out). These show that a ridge, from edge to edge through the center of the sample, exists along the b-axis. Superimposed upon this is a surface roughness with an average peak to peak amplitude of about one micron, but with occassional peaks projecting 3-4 microns above the ground level.

Figures 7 and 8 show roughness plots of the bottom sample used in the 10° orientation run. Surface roughness with an average peak to peak amplitude of 2-3 microns is present. Numerous individual peaks projecting over 5 microns above the ground level can be seen.

Figures 9 and 10 show roughness plots of the upper sample used in the 10° orientation run. A hump reaching a height of about 15-20 microns above the edge is present. Superimposed upon this is a general roughness with an average peak to peak height of a few microns, but with individual peaks of height greater than 5 microns.

The data are shown in Figure 11. These were obtained at a vacuum of about 2×10^{-10} mm Hg, at room temperature, and with previous sample bakeout for about one hour at temperatures in excess of 500°C. The samples contacting along the (001) plane were first oriented with an angle of 80° between respective a-axes, and then with an angle of 10° between these axes. It can be immediately noted that for the smaller loadings no adhesion is detectable (e.g., the adhesion force is less than 20μ gm). As load force

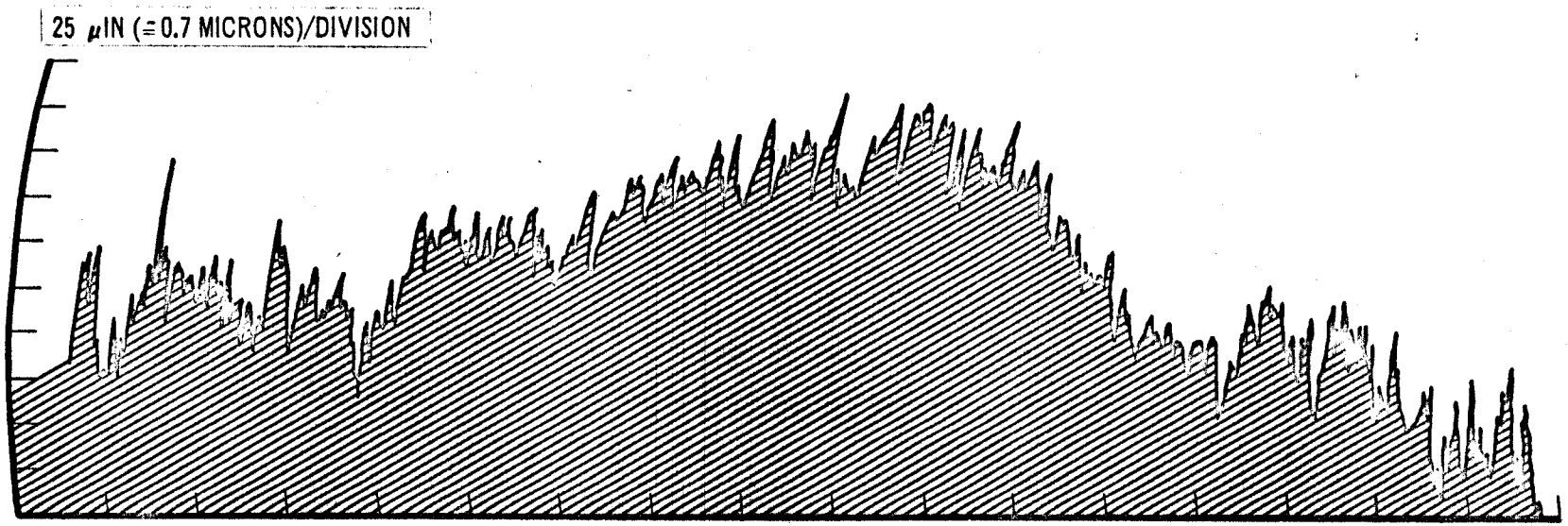

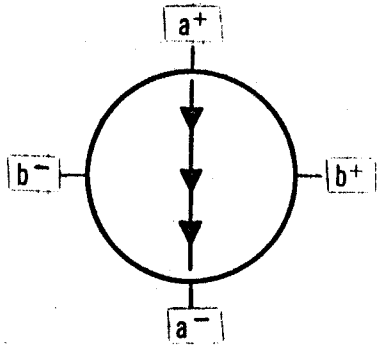

Figure 4

Run #1 Orthoclase (001)/Orthoclase (001) Top Sample, Surface Roughness Along A-Axis

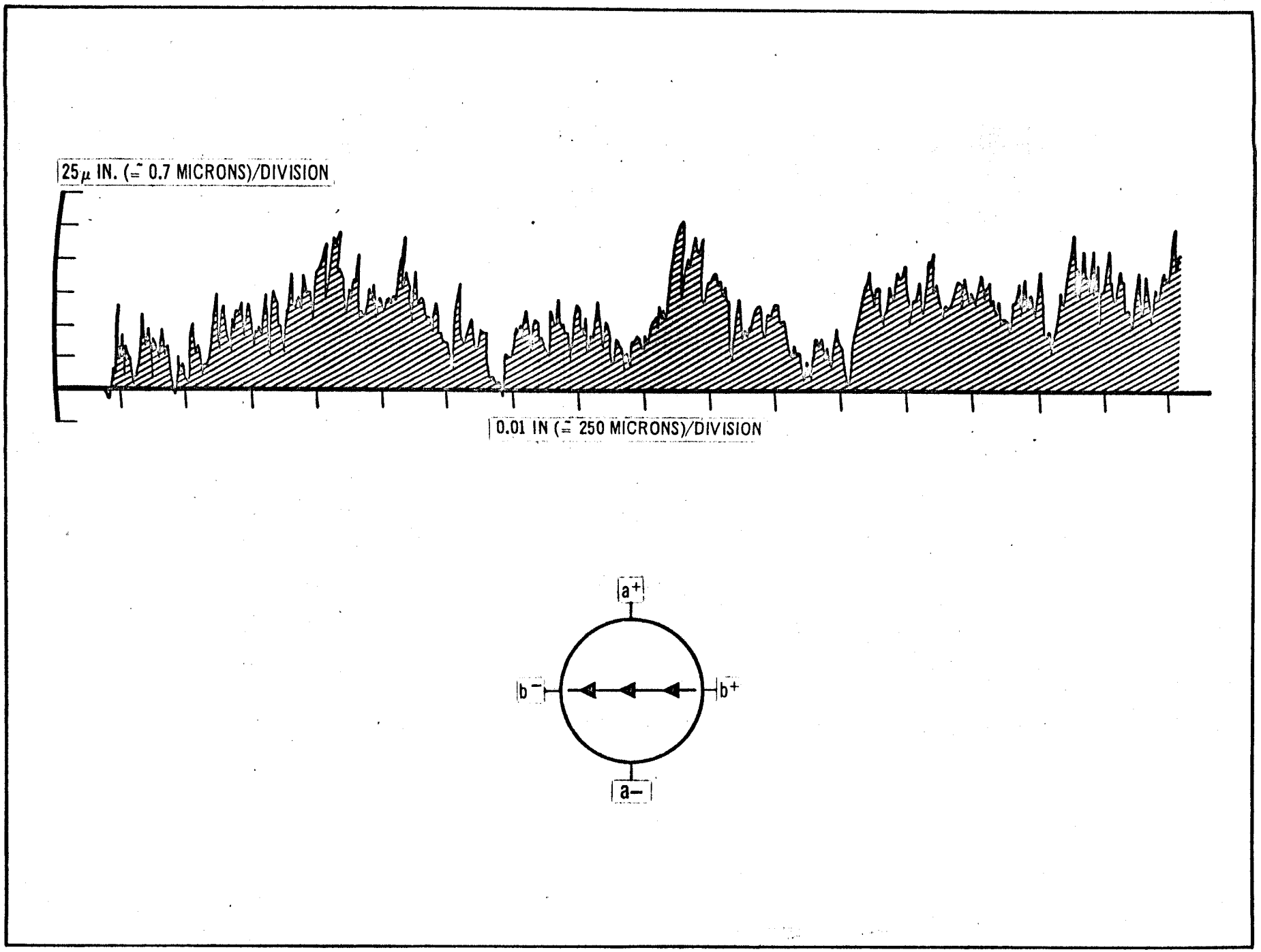

Figure 5

Run # 1 Orthoclase (001)/Orthoclase (001) . Top Sample Surface Roughness Along B-Axis

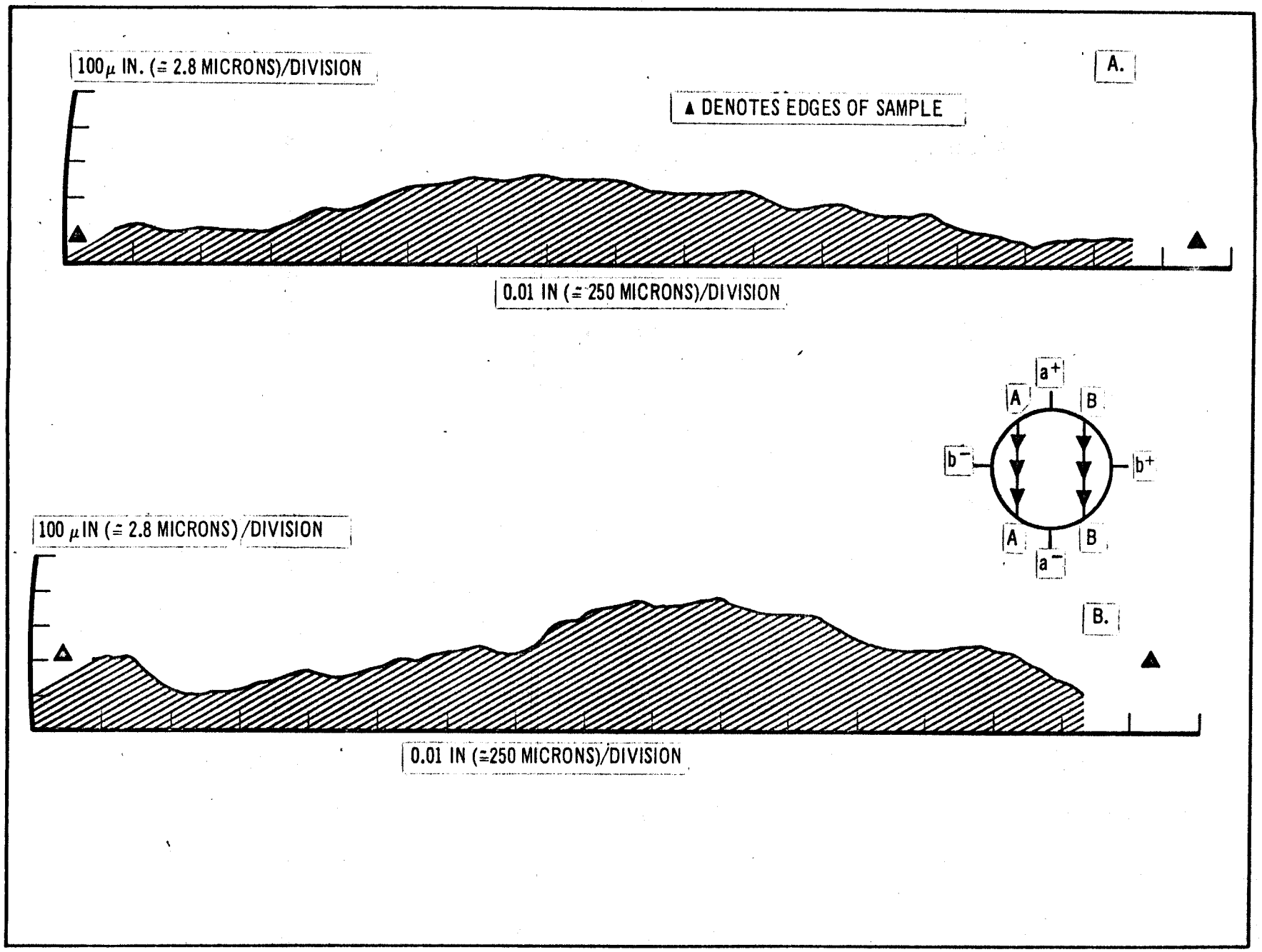

Figure 6

Run #1 Orthoclase (001)/Orthoclase (001) Top Sample Large Scale Surface Roughness Along A-Axis

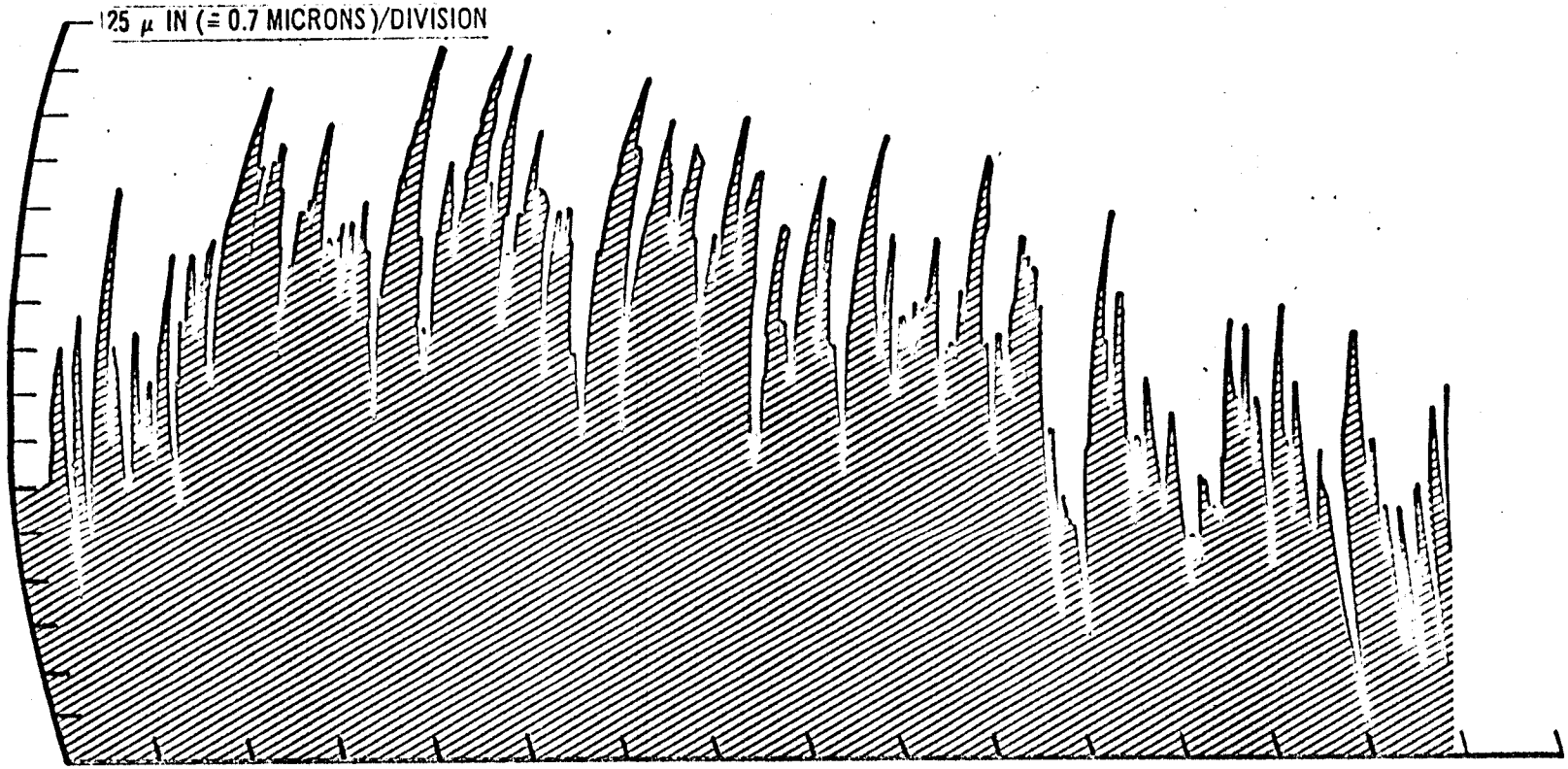

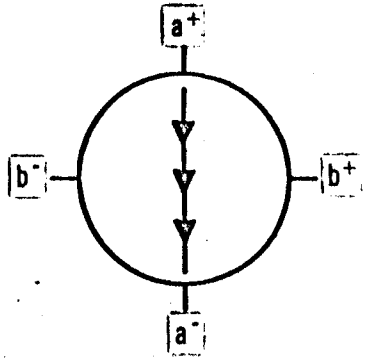

Figure 7 Run # 2 Orthoclase (001) Bottom Sample Surface Roughness Along A-Axis

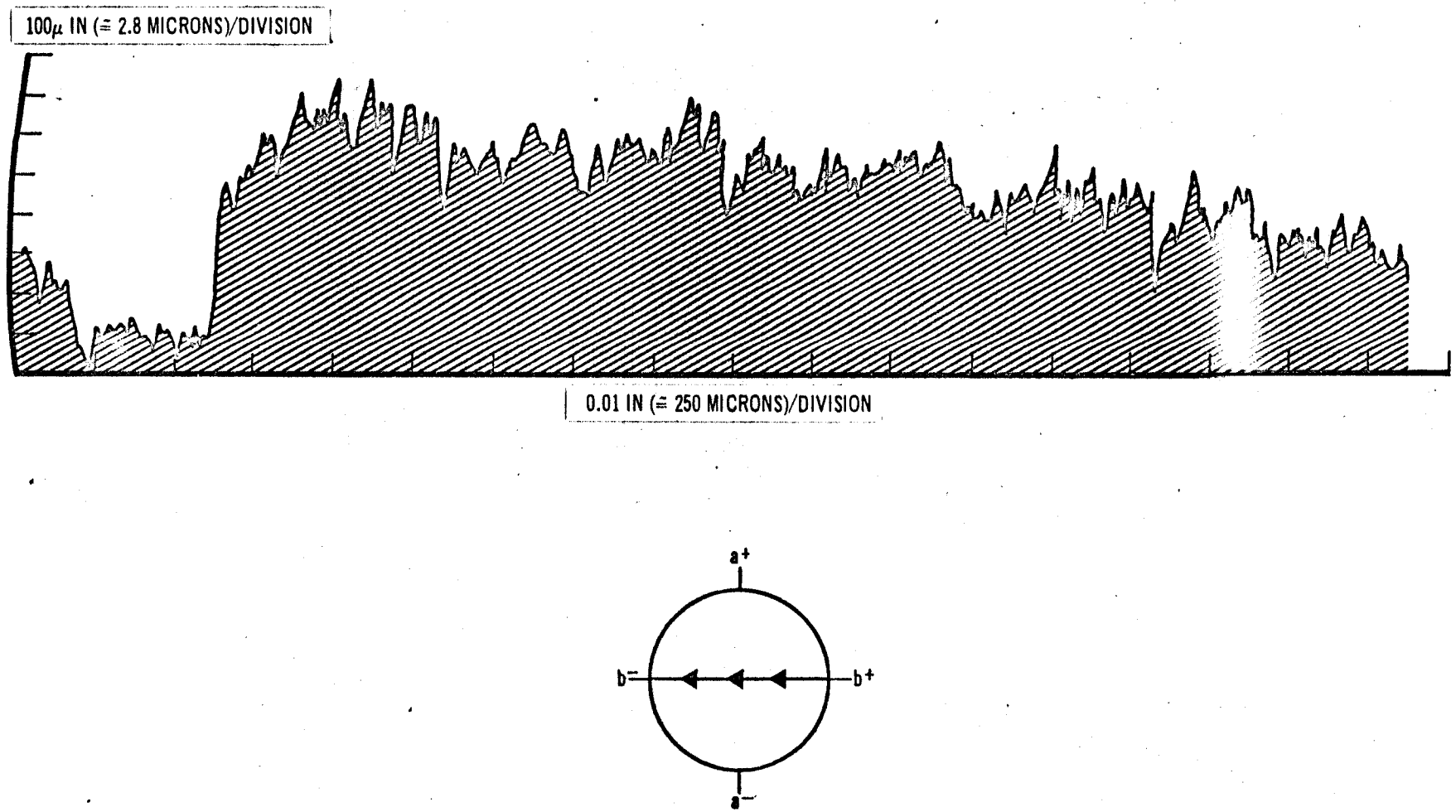

Figure 8 Run #2 Orthoclase (001)/Orthoclase (001) Bottom Sample Surface Roughness Along B-Axis

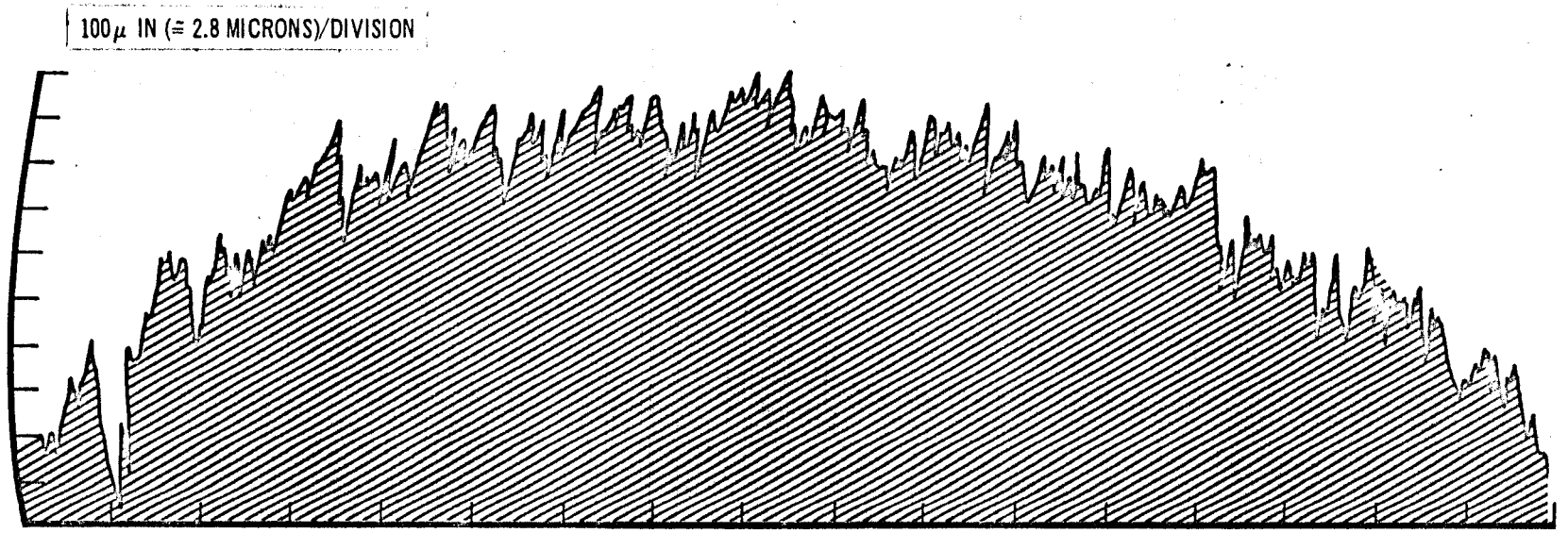

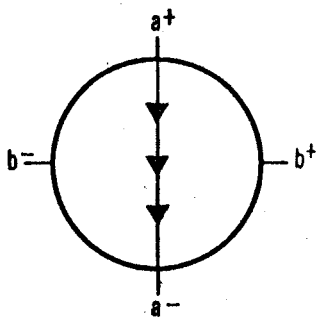

Figure 9

Run # 2 Orthoclase (001)/Orthoclase (001) Top Sample Surface Roughness Along A-Axis

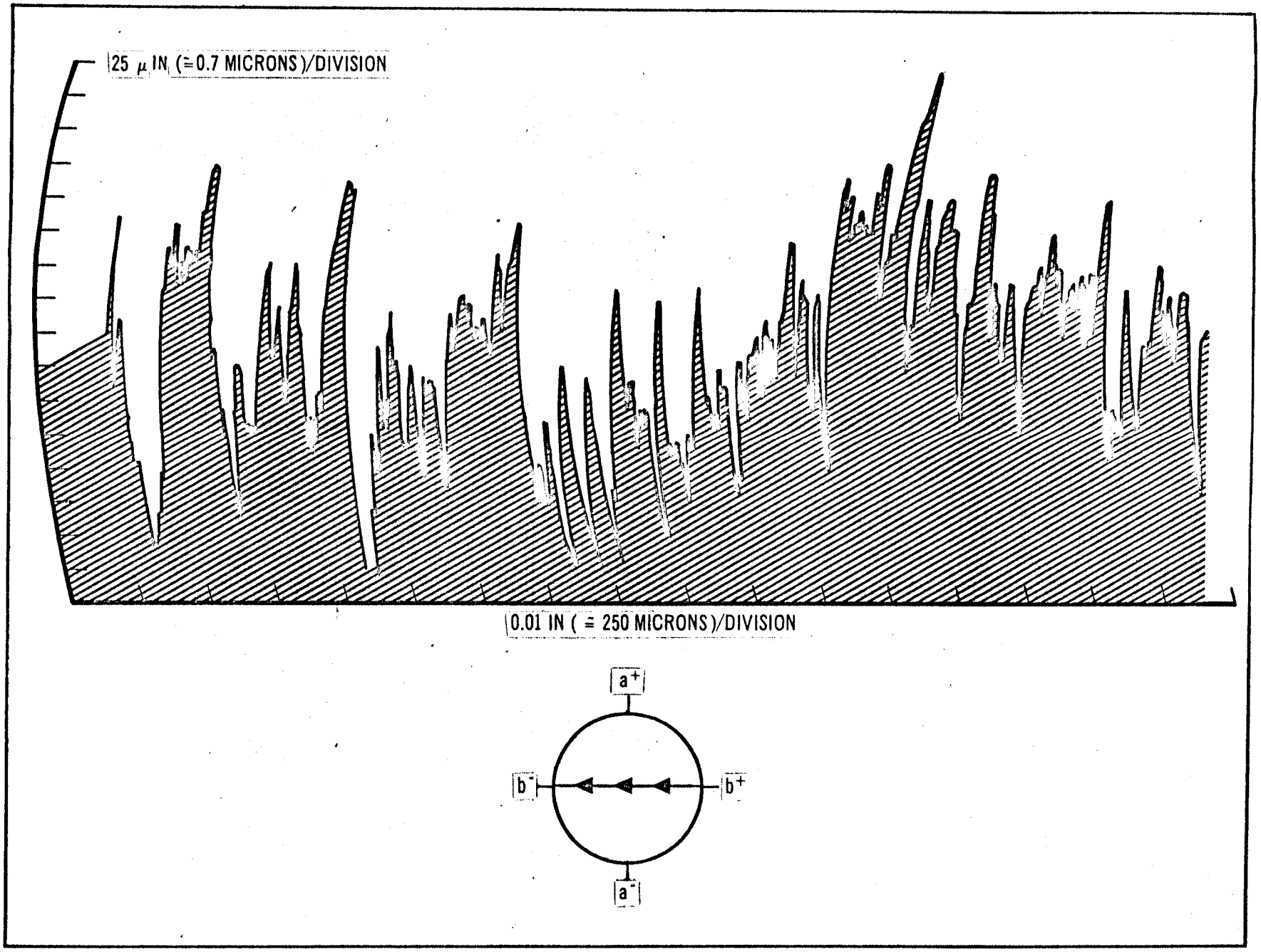

Figure 10

Run #2 Orthoclase (001)/Top Sample Surface Roughness Along B-Axis

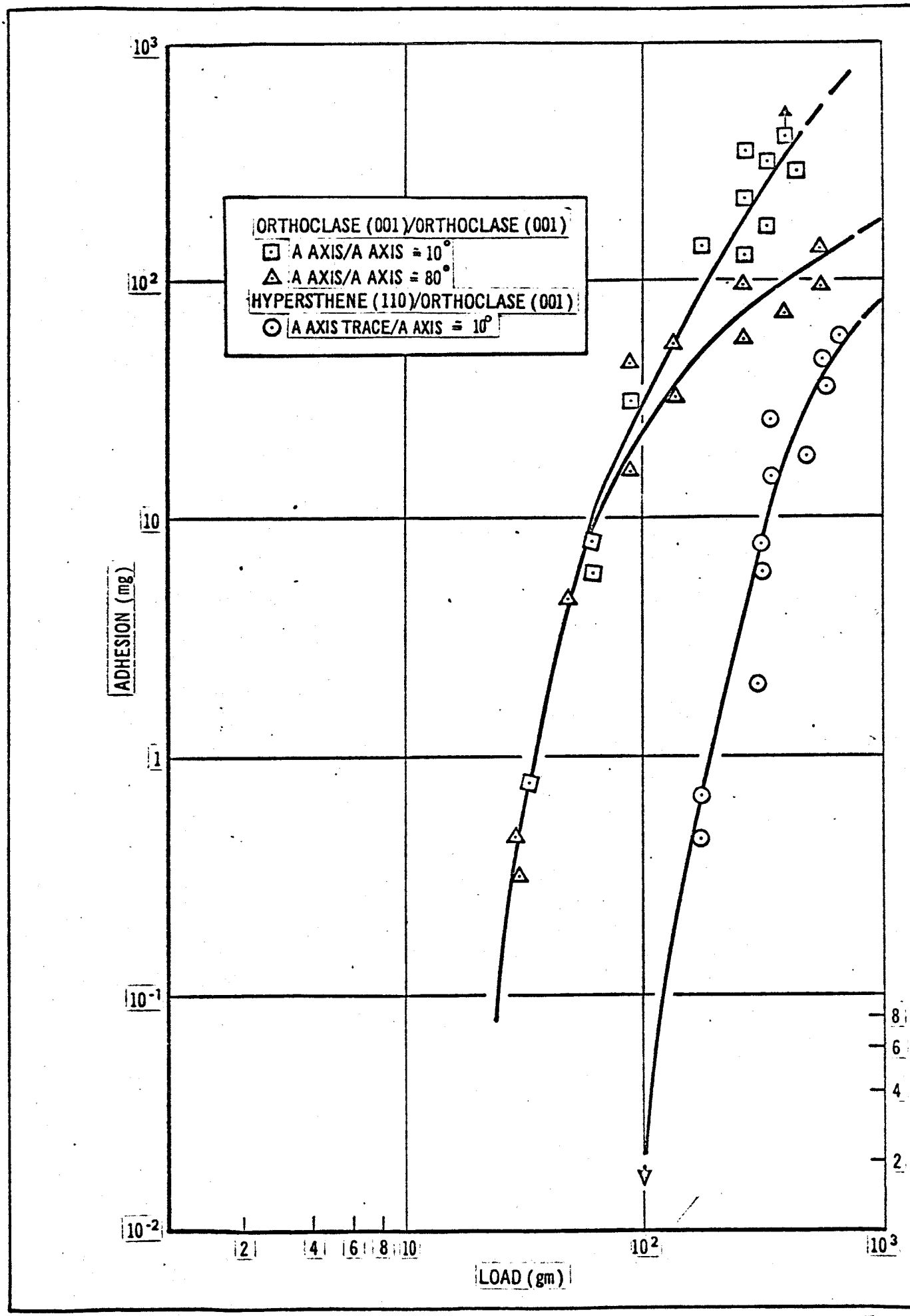

Figure 11 Adhesion Force Vs. Load for Various Silicates

is increased an extremely rapid increase in the adhesion occurs initially, followed then by a slower increase. The plots for the two different crystallographic orientations are similar during the initial rapid rise with increasing load, but thereafter the respective adhesions diverge rapidly, the adhesion for the orientation closer to atomic match being considerably larger (for the 10^{o} orientation case and with loads greater than about 500 gm the adhesion force exceeded that measurable with the microbalance and it was necessary to tap the base plate supporting the bottom sample in order to separate the samples). The magnitudes of the adhesion forces measured were surprisingly large, considering the roughness of the contacting surfaces.

Following each run the vacuum system was brought up to atmospheric pressure with dry nitrogen and attempts made immediately to detect adhesion under these conditions. Within the first few minutes, using load forces greater than 500 gm, adhesion forces of a few milligrams were detected. These, however, quickly disappeared and subsequently no adhesion could be detected at any loading. In addition, attempts were made to measure adhesion during the pumpdowns prior to each run. These attempts were made at pressures of 10^{-3} mm Hg and 10^{-6} mm Hg. In no case was any indication of adhesion obtained.

Following each run, the sample surfaces were studied by means of a Leitz petrographic microscope. Flakes of orthoclase were found on each surface; these having broken loose (along the cleavage planes) during the run. It was not possible to determine whether these were produced through the mechanical action of the loading or through the action of the adhesion. The flakes appeared to be adhering to the surfaces, but we were not able to determine

the nature of this adherence. Due to the similarity of the two surfaces, it was not possible to determine whether transfer of material between the surfaces had occurred. Photomicrographs of these surfaces will be included in the first annual report for this study.

b. Orthoclase (001) vs Hypersthene (110)

Hypersthene is a member of the Pyroxene Group of minerals and has a composition of $(Mg,Fe)_2\ Si_2O_6$. It belongs to the orthorhombic crystal system and has a Mohs hardness of between five and six. It is closely related to enstatite, differing principally by the presence of additional iron. It, along with enstatite, is a common constituent of basic and ultrabasic igneous rock and the stony phase of meteorites. The source locality for the hypersthene used in this study is Bamle, Telemark, Norway.

The hypersthene (110) plane is a "good" cleavage plane and represents the direction along which fracture, during comminution, occurs most readily.

The surface roughness profiles for the two samples are shown in Figures 9, 10, 12, and 13. Figures 9 and 10, for orthoclase, have been discussed previously. Figures 12 and 13, for hypersthene show a surface roughness averaging 1-2 microns in height. The figures also show the presence of some surface cracks.

The data are shown in Figure 11. These were obtained at a vacuum of about 2×10^{-10} mm Hg, at room temperature, and with previous sample bakeout for about one hour at temperatures in excess of $500^{\circ}C$. The samples were oriented

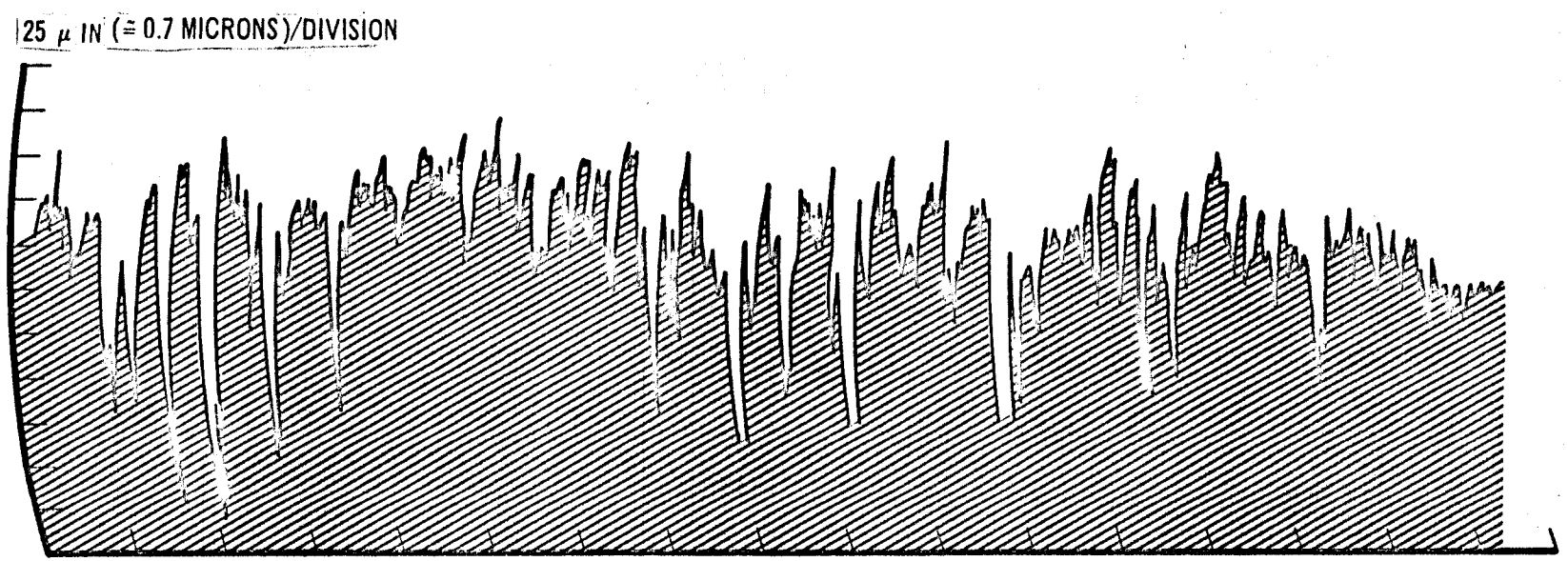

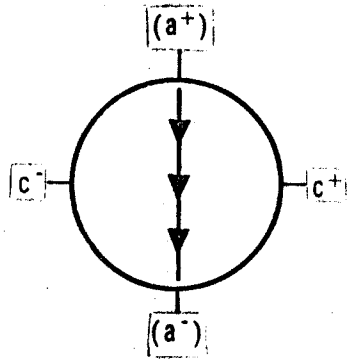

Figure 12

Run #3 Orthoclase (001)/Hypersthene (110) Top Sample (Hypersthene) Surface Roughness Along A-Axis Projection

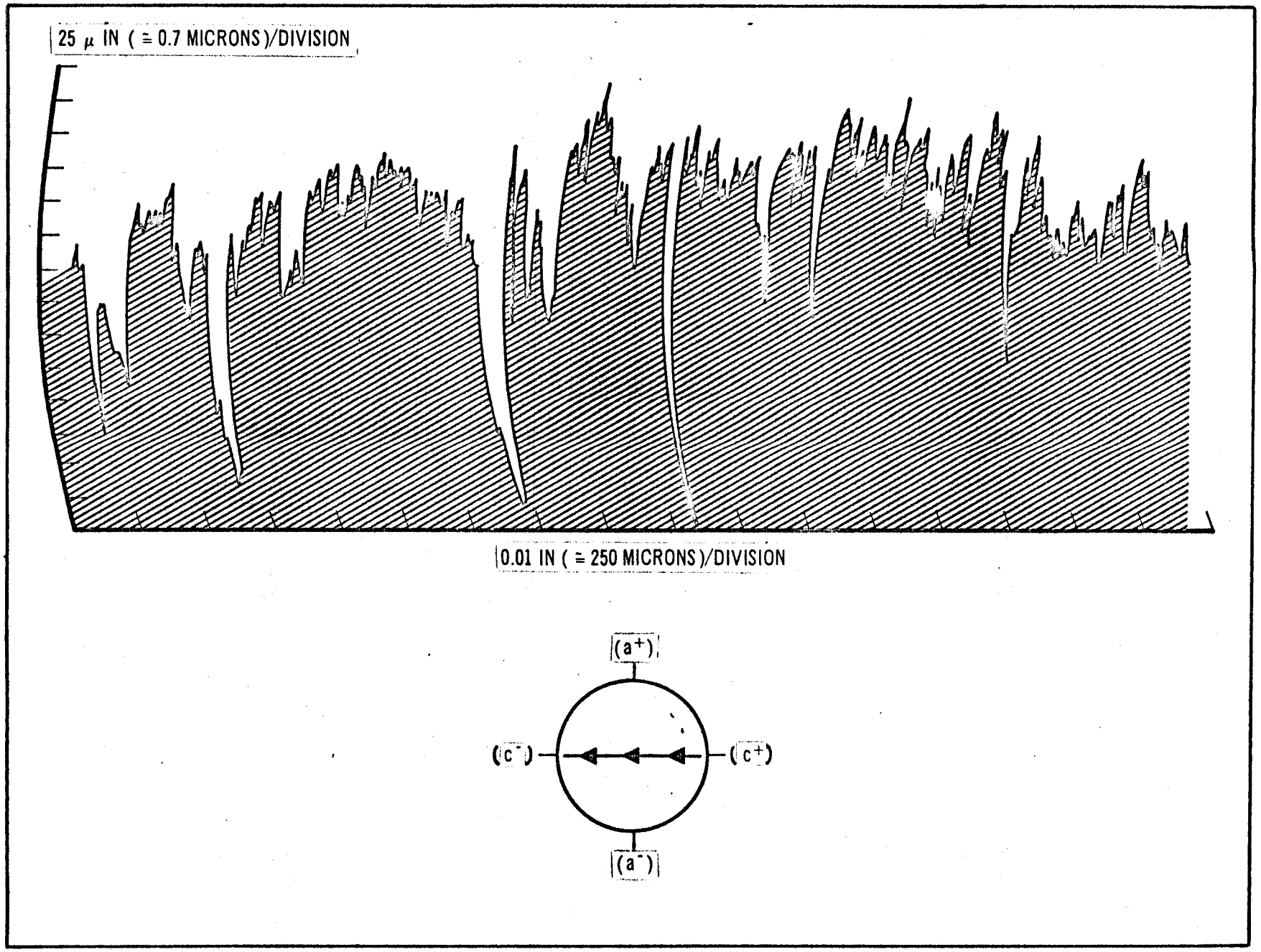

Figure 13

Run # 3 Orthoclase (001)/Hypersthene (110) Top Sample (Hypersthene) Surface Roughness Along C-Axis

6. The hypersthene is not as hard as the orthoclase so that the transfer of material is in the proper direction.
7. The dark deposit occurred principally on surface projections.
8. The dark material could not be removed by physical brushing and rubbing of the surface.

It is concluded, tentatively, that the transfer of hypersthene to the orthoclase face is a result of the action of adhesion forces, and hence that the normal silicate bonding forces were acting at vacuum.

c. Orthoclase (001) vs Albite (001)

Albite is a member of the Feldspar Group of minerals and has a composition of approximately NaAl Si_3O_8. In particular, it is a plagioclase feldspar forming one end member of an isomorphous series varying in composition from that of albite to that of anorthite ($CaAl_2$ Si_2O_8). It belongs to the triclinic crystal system and has a Mohs hardness of six. The plagioclase feldspars are common constituents of igneous rock. Albite is found principally in the acidic rocks, anorthite principally in the basic varieties; both are found in the stony phase of some meteorites. The source locality for the albite sample used is Madagascar.

The albite (001) plane is a "perfect" cleavage plane and represents the direction along which fracture, during comminution, occurs most readily.

The surface roughness profiles for the two samples are shown in Figures 9, 10, 14, and 15. Figures 9 and 10 have been discussed previously.

so that the orthoclase a-axis was about 45° from the hypersthene c-axis. For the smaller loadings no adhesion was detected, but as the loading is increased an extremely rapid increase in the adhesion occurs. It should be noted that the adhesion obtained, for a given load, is much less than that obtained from the contacting orthoclase surfaces.

Following this run the vacuum system was brought up to atmospheric pressure with dry nitrogen and attempts were made immediately to detect adhesion under these conditions. None was detected.

The sample surfaces were then studied by means of the petrographic microscope. Flakes of orthoclase and hypersthene were found on both surfaces. In addition, dark material was found to be "smeared," in small amounts, over the orthoclase surface. A photomicrograph of this will be included in the first annual report for this study. However, it is worth noting the following points at this time:

1. This dark material was not present on the orthoclase prior to the run.
2. This is the first time such an effect has been noted, which indicates strongly that this is not a contaminent from the vacuum system.
3. This is the only run to date in which a light colored mineral has been contacted with a dark mineral; in all other runs minerals of similar color have been used so that this effect, if representing transfer of material between the surfaces, could not have been detected.
4. Study of the deposit indicates it is hypersthene.
5. The deposit only occurs in those regions for which the roughness plots indicate that intimate contact between the surfaces could have occurred.

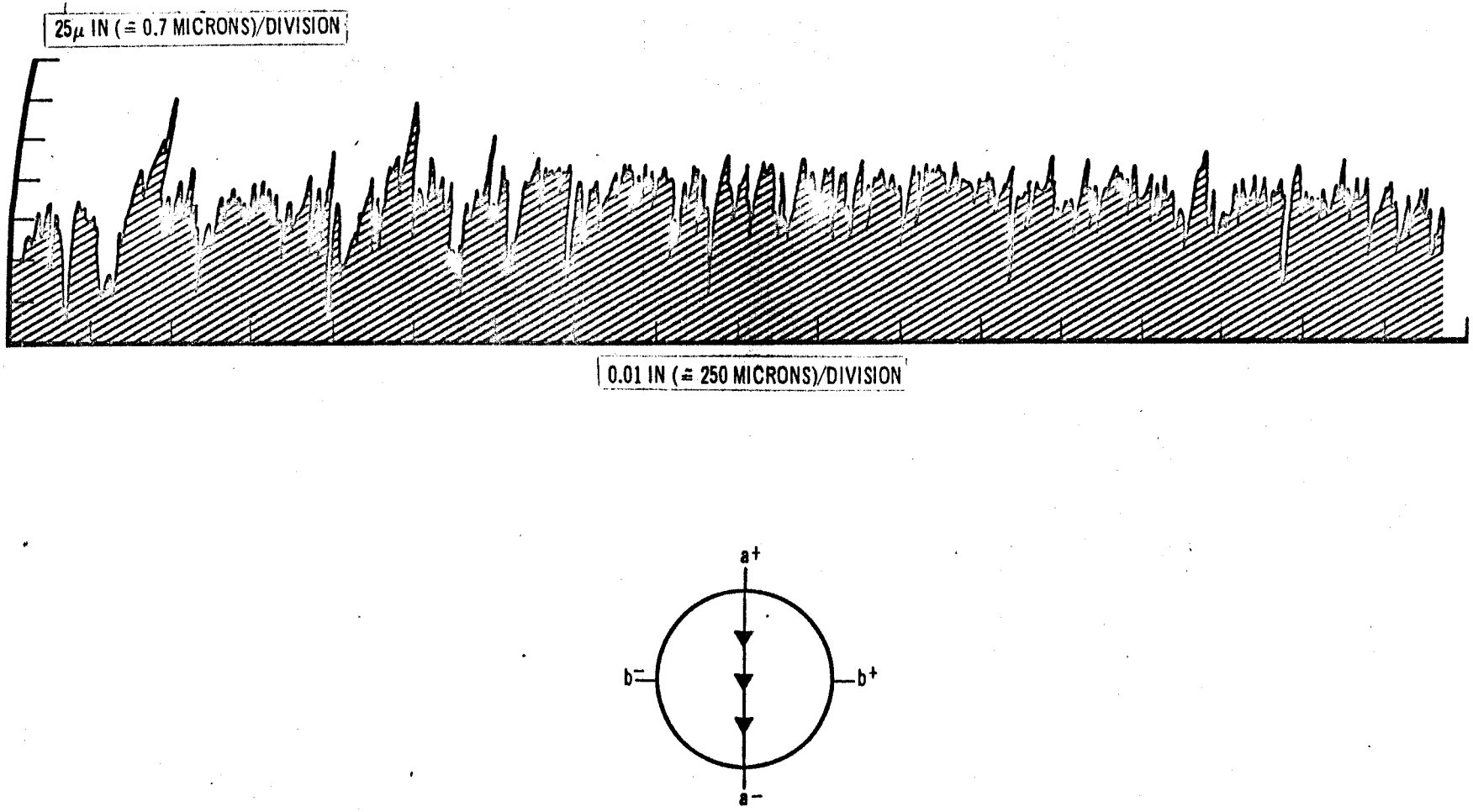

Figure 14

Run # 4 Orthoclase (001)/Albite (001) Albite Sample Surface Roughness Along A-Axis

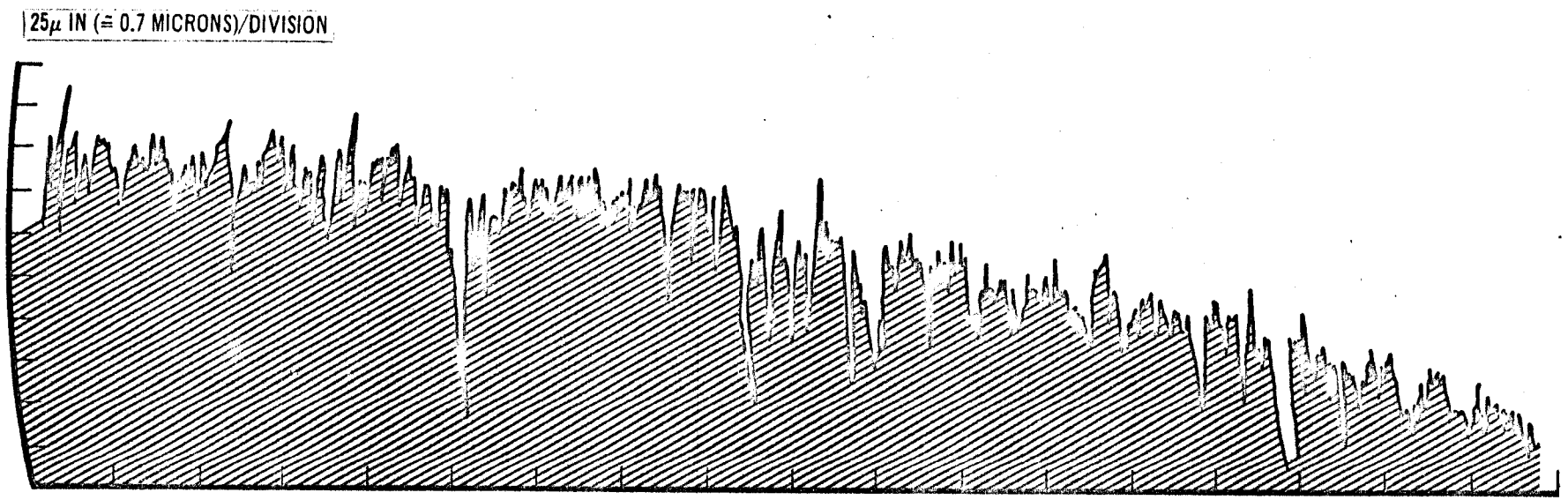

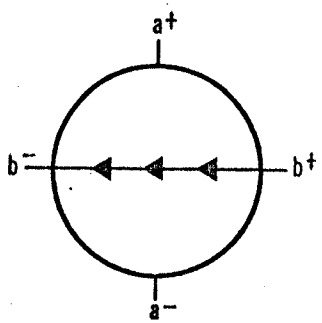

Figure 15

Run # 4 Orthoclase (001)/Albite (001) Albite Sample Surface Roughness along B-Axis

Figures 14 and 15 show the albite surface. It is immediately evident that this surface is much smoother than any of the others studied. The roughness peak to peak averages less than one micron.

The data are shown in Figure 16. These were obtained at a vacuum of about 3×10^{-10} mm Hg, at room temperature, and with previous sample bakeout for about one hour at temperatures in excess of $500^{\circ}C$. The samples were oriented so that the respective b-axes were about 10° from match.

It is seen immediately that the nature of the adhesion-load curve is quite different from that of the sample pairs studied previously. In particular, measurable adhesion is present at zero load; and the adhesion increases quite slowly with increasing load. Also, the values obtained for the higher loads are orders of magnitude less than obtained in the previous runs. This behavior was quite surprising in the light of the previous data. The implications of this behavior are discussed in a following section. It is worth noting here, however, that the albite sample used had much less surface roughness than the other samples.

After completion of this run, the system was let up to dry nitrogen. A slight indication of residual adhesion under load was obtained, but this disappeared completely within a few minutes.

d. Orthoclase ($00\bar{1}$) vs "Pure" Aluminum

This run represents the first experiment with a silicate contacting a non-silicate, e.g. a metal. The aluminum was furnished by Johnson, Matthey and Co.,

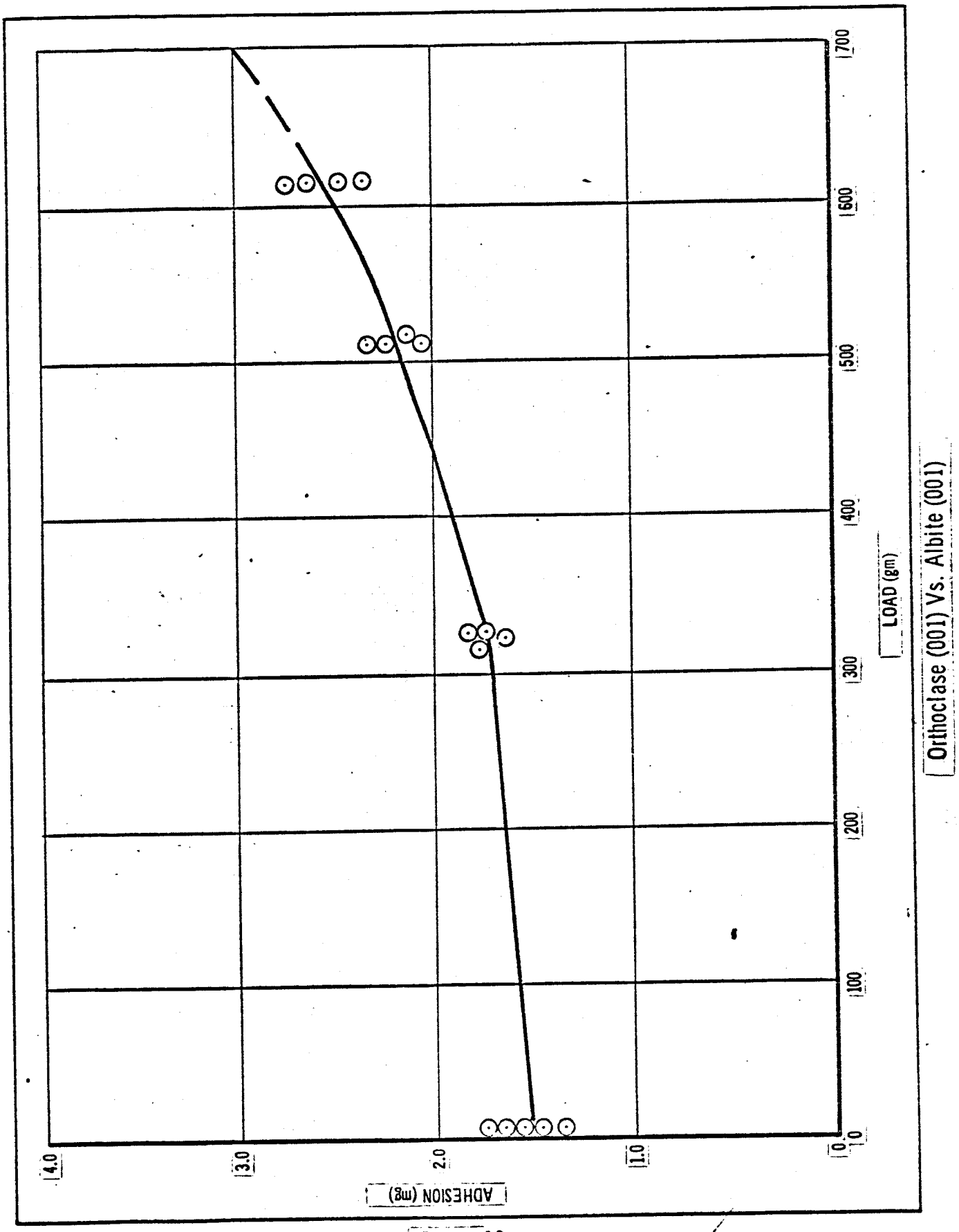
Orthoclase (001) Vs. Albite (001)
LOAD (gm)
0.10
100
200
300
400
500
600
700
ADHESION (mg)
4.0
3.0
2.0
1.0

Figure 16

Limited, London, England, A spectrographic analysis of the sample was made by the supplier. The impurities present are as follows:

Element	Estimate of Quantity Present (parts per million)
Mg	30
Fe	5
Si	3
Cd	2
Cn	1
Na	1
Ag	<1

Forty-three additional elements were specifically sought for but not detected.

Surface roughness plots for the aluminum have not as yet been obtained. These will be included in the forthcoming annual report. Surface roughness plots for the orthoclase are given in Figures 9 and 10.

The data obtained are shown in Figure 17. These were obtained at a vacuum of about 3×10^{-10} mm Hg, at room temperature, and with previous sample bakeout to temperatures somewhat in excess of $400^{\circ}C$. The adhesion vs load plot is shown as having two branches. It is of interest to note the events which led to showing such a separation.

The vacuum system is suspended from "soft" springs in order to reduce vibration problems. Even though this isolation system performs satisfactorily,

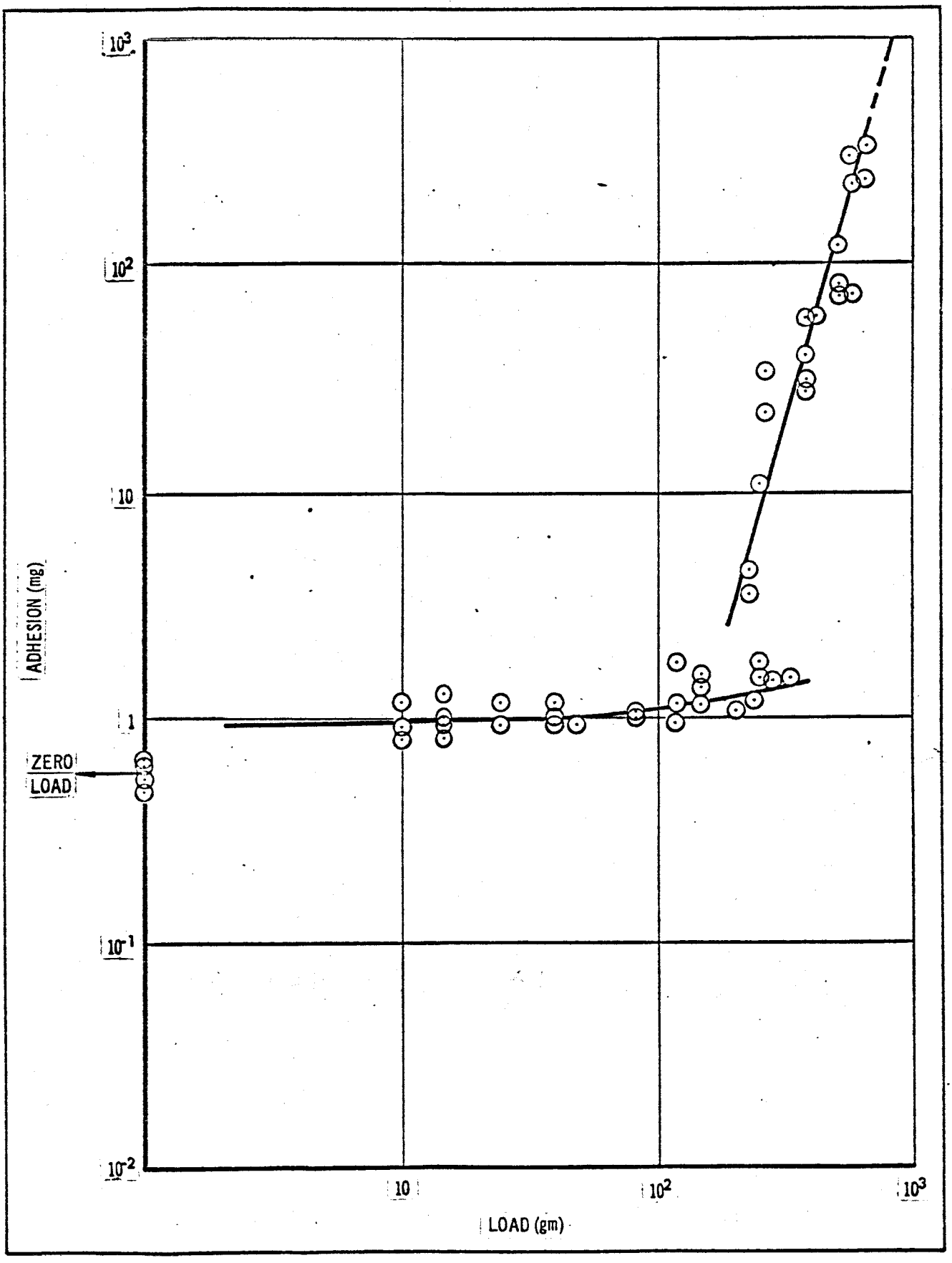

FIGURE 17 Pure Aluminum Versus Orthoclase (001)

it has been noted that the system is still affected sufficiently by certain large amplitude transients (slamming of doors locally, etc.) to compromise the data obtained when these transients occur. Through experience in operation of the experiment, we have been able to develop the ability to tell, quite well, which sounds affect the system and which apparently do not. During this run, as with all runs, data are discarded if a disturbance has been noted during the measurement. This technique has worked well for previous runs, but in this case it was found that for load forces between 200-350 gm many of the adhesion data appeared low, even though no disturbing noise was detected. It was thought at first that some, as yet unrecognized, noise source was acting, and accordingly these data were discarded. However, except for the data being low, there is no real justification for doing this. In fact, when plotted, these data appear to be a logical extension of the data obtained at lower load forces. Also, it can be noted from comparison with Figures 11 and 16 that the lower segment of the orthoclase/aluminum curve is similar to that obtained for orthoclase/albite and that the upper segment bears some slight resemblance to the orthoclase/orthoclase and orthoclase/hypersthene curves. Because of these observations, it is tentatively accepted as a working hypothesis that the separation of the adhesion/load curve into two branches is real. The implications of this are discussed in the following section. It is worth noting here, however, that no indications of a continuance of the lower curve beyond 350 gm was obtained.

Following this run, the system was brought up to atmospheric pressure with dry nitrogen. Adhesion measurements were attempted and it was found that

adhesion was still present. Measurements were carried out over a period of about eight hours, each data set spaced about one hour apart. At the end of this period, measurable adhesion was still present. Under zero load it showed a tendency to decrease with time, the first measurement immediately after admitting dry nitrogen giving a value of about half the vacuum value, the adhesion (under zero load) then dropping in magnitude to about one-tenth the vacuum value within the first few hours. After this period load forces were applied. It was found that: 1) application of load immediately raised the magnitude of the zero load values, 2) forces comparable to those represented by the lower branch of the vacuum adhesion curve were detected, and 3) the upper branch had apparently disappeared.

By bringing the samples out of contact and then slowly into contact through varying the current in the microbalance, it was found that a long range attractive force was present. This is the first time such a force has been detected, even though checks for the presence of long range forces have been made a number of times during all runs. It is of interest to note that for this run no indications of a long range attractive force were detected while at vacuum. Implications of these data are discussed in the following section.

Studies of the contacting surfaces with the petrographic microscope are underway. These will be discussed in the next report. However, preliminary scans indicate that a small amount of the aluminum is adhering to the orthoclase and that some disruption of the aluminum surface has occurred.

2.4.3 Nature of the Forces Acting

2.4.3.1 Preliminary Discussion

The forces which could cause adhesion of silicates at the lunar surface have been discussed in previous quarterly reports. In brief, they are: 1) homogeneous surface charging, 2) mosaic surface charging, 3) the dispersion, or London-Van der Waals forces, and 4) the normal silicate bonding forces (ionic-covalent). In addition to these, there are forces (and effects) which could conceivably affect the data obtained in the present study and hence are worth noting. These are effects produced through application of electromagnetic fields in the generation of the loading force, residual magnetism, and wedging (this later could conceivably operate on the moon). It is worth discussing these additional forces, before beginning a detailed analysis of the data, to show that these possible effects are not contributing appreciably to the adhesion measured.

The presence of an electromagnetic field during the sample loading can produce polarization in the samples (those such as the silicates which are dielectrics). This polarization can, however, be immediately excluded as causing the adhesion since: 1) theoretically it should disappear upon removal of the field, 2) no adhesion is detected for the silicates in dry nitrogen except briefly, immediately after admission of the nitrogen, and 3) in those cases where adhesion is detected at zero load, there is a smooth transition between this and the loaded cases.

Residual magnetism originally gave trouble. It was found that with repeated

applications of the magnetic field the "non-magnetic" stainless steel (304) became magnetized to the degree that it was easily detectable and interfered with the adhesion measurements. A number of other "non-magnetic" stainless steels were then tried in air, and none were found which would be suitable for use. This problem was resolved by replacing the plate on thich the lower sample sits by a copper plate. Additional problems arose, on occasion, by the mineral samples being magnetic. This magnetism, undetectable by standard techniques, is easily observed and measured by the microbalance. This problem has been resolved by exposing the samples to a strong magnetic field in air and seeing whether the microbalance could detect any residual magnetism.

In summary, it can be stated that residual magnetism is not contributing to the measured adhesion forces.

Wedging could occur between rough surfaces by the application of load, the load forcing the surfaces closer and by lateral micro-displacements causing an interlocking and wedging together of the asperities. That this is not an appreciable contributor to the measured adhesion is demonstrated by the quick decay and disappearance of the adhesion (under load) when the system is brought up to dry nitrogen.

2.4.3.2 Homogeneous Surface Charging

It is well known that silicates can acquire a net positive or negative surface charge, and that this charge can play a role in the coagulation of aerosols. In any adhesion study it is important to determine the degree to which such charging can contribute to the forces measured. It has been

determined in this study, on rather good experimental grounds, that these forces do not contribute to the measured adhesion between the silicates. Evidence has been uncovered, however, that homogeneous surface charging could play a significant role in contacts between silicates and metals.

The arguments against homogeneous surface charging contributing significantly to the measured adhesion for silicates are as follows:

1) Homogeneous surface charging produces long range forces. No evidence for the presence of long range forces has been uncovered. This has been investigated by separating the samples and then bringing them slowly toward contact by varying the microbalance current.
2) After each loading and subsequent separation, the samples were immediately brought back into contact at zero load. In no instance was a change in the zero load adhesion detected.
3) No adhesion was detected at 10^{-3} and 10^{-6} mm Hg; also adhesion quickly disappeared when the system was backfilled with dry nitrogen (this argument is not conclusive by itself, but lends support to the previous arguments).
4) Maximum adhesion has been detected for those surfaces which are most similar, e.g., the contacting orthoclase (001) planes. Surface charging can be produced by processes external to the surface such as incident electromagnetic or corpuscular radiations, or by the differing work functions of the surfaces. (It has been postulated that adhesional charging could occur, but this is not generally believed to be significant.) It is reasonable to exclude external

processes from being operative to any significant degree in the present experiment. Hence, if homogeneous surface charging is responsible for the adhesion, the adhesion should be greatest for those surfaces which are most dissimilar on an atomic-molecular scale.

5) Indications have been obtained that material transfer between the contacting surfaces has occurred.

The situation is somewhat different for the run involving orthoclase (001) contacting aluminum. Here, as noted previously, long range forces have definitely been detected at atmospheric pressure in dry nitrogen. Rough calculations of the contact potentials required, and comparison of these with those which have been determined by various investigators for semi-conductor/metal contacts, indicate that homogeneous surface charging could account for the forces detected in dry nitrogen (a few hundred micrograms to about one milligram). However, they could not account for the large forces measured in vacuum (upper branch of the adhesion/load plot given in Figure 17.

One troublesome point remains, however: long range forces were detected in dry nitrogen, but definitely not at vacuum. It is not clear why this should be so, the only possible explanation which comes to mind being that perhaps the admission, and adsorption, of nitrogen causes changes in the nature of the surfaces which affect the contact potential. Some indications of changes in contact potential as a function of composition of the surrounding atmosphere have been obtained by various investigators studying semi-conductors. However, further work is required before anything

definite can be said about the present case.

2.4.3.3 Mosaic Charging

Of all the possible forces which may produce adhesion, determination of the presence or absence of those forces resulting from mosaic charging is the most difficult. Mosaic charging was first postulated by Derjaguin to explain the anomalously high attractive forces detected by Overbeek and Sparnay (references cited in previous quarterly report). According to Derjaguin, no surface being perfect with respect to atomic arrangement, lack of localized impurities, etc., a mosaic distribution of charges (of opposite signs) could be generated, with the net surface charge remaining zero. If a certain amount of surface mobility of these charges is allowed, then forces could act between two dielectrics brought into close proximity or contact. Because of the mosaic distribution of these charges, the range of effectiveness of the forces produced would be orders of magnitude less than those produced by homogeneous surface charging, but greater than the range of effectiveness of the dispersion forces (London-Van der Waals). To the present writer's knowledge, the presence of mosaic charging on a micro-scale has never been experimentally verified. However, the possibility of their presence cannot be excluded.

What makes it difficult to evaluate the role such charges may play is that for almost any adhesion force detected, one can postulate a given distribution of surface charging which could produce the required force. Derjaguin does note that if good reproducibility is obtained between successive measurements it would appear that mosaic charging is not playing a significant role in

the adhesion. The only additional ways, feasible in the present study, which could possibly provide the necessary discrimination are the detection of a crystalline orientation dependence (for given faces in contact) and the detection of adhesion-produced surface disruption. These, however, are rather indirect techniques since they provide definitive information only if crystalline orientation effects and/or surface disruption can be demonstrated.

Some indications that mosaic charging is not contributing significantly to the measured adhesion have been obtained. These are as follows:

1) The two orthoclase runs for the same crystal faces in contact, but with different orientation of the axes indicate a crystalline orientation dependence.
2) Maximum adhesion has been obtained for contacting surfaces most alike.
3) Some evidence that adhesion-produced material transfer between the contacting surfaces occurs has been obtained.
4) Good reproducibility has been obtained for the orthoclase/albite run. The scatter for the previous runs is considerably larger, but this appears to be due primarily to faults in the measurement techniques which have since been corrected.
5) Adhesion between the silicates rapidly disappears when the system is brought up to dry nitrogen (this argument, by itself, will never be completely convincing, but taken with the other arguments it aids in the discrimination).
6) Immediately after each load application, adhesion is measured at zero load. No significant effect of the previous loading upon the

adhesion at zero load (for the silicates) has been detected.

In summary, indications that mosaic charging is not playing a significant role in the adhesion have been obtained. However, many more data are required before a definitive conclusion can be reached.

2.4.3.4 Dispersion and Ionic-Covalent Forces

Dispersion (London-Van der Waals) forces have a range of effectiveness much greater than that of the ionic-covalent forces, but less than that for the postulated mosaic-charge-produced forces. The force-distance relationships for these dispersion forces have been calculated theoretically and verified experimentally (for surface separations greater than a tenth of a micron). This experimental verification of theory is of particular interest since it indicates that even though the theory was developed for molecular solids, it is more or less applicable to silicates (most of the experiments were performed upon quartz and fuzed silica).

For two parallel plates, the equations expressing the dispersion force behavior are

$$F\ (\text{dynes cm}^{-2}) \cong \frac{2.6 \times 10^{-15}}{h^3\ (\text{cm})} \quad h < 200\text{A}^\circ$$

$$F\ (\text{dynes cm}^{-2}) \cong \frac{10^{-19}}{h^4\ (\text{cm})} \quad h > 2000\text{A}^\circ$$

where F = attractive force per unit area and h = separation of the surfaces.

The magnitude of the adhesion produced by dispersion forces is then, for various surface separations (assuming atomically flat surfaces):

h (microns)	F (dynes cm^{-2})	Experimental Verification
2×10^{-4} ($2A^{\circ}$)	3×10^{8}	No
5×10^{-4} ($5A^{\circ}$)	2×10^{7}	No
10^{-3} ($10A^{\circ}$)	2.6×10^{6}	No
10^{-2} ($100A^{\circ}$)	2.6×10^{3}	No
10^{-1}	1.5	Yes
0.5	1.6×10^{-2}	Yes
1.0	10^{-3}	Yes
2.0	6×10^{-5}	No

Unfortunately, for the relatively rough surfaces being used in the present study, the best that can be expected from this tabulation is that it can provide indications as to the possible magnitudes of the dispersion force produced adhesion. This table will, however, be used to a considerable degree as the study progresses. For the present, it will be used only to note that for the largest adhesion forces measured to date, $F_a \geq 0.4$ gm, if the sample surfaces were optically flat, the samples would have to be separated by less than $100A^{\circ}$ if only dispersion surfaces were acting (total surface area $\cong 0.3$ cm^2). On the other hand, if certain parts of the surfaces were in intimate contact ($\approx 2A^{\circ}$ separation), the total required area of intimate contact would be $\approx 10^{-6} cm^2$ (after removal of the applied load). This is considerably in excess of that to be expected from simple elastic or plastic deformation theory. However, it could be realized, if under load, the contacting surfaces move much closer together (mate better).

The evidence collected to date which indicates that the dispersion forces may not in general be the primary forces responsible for the observed adhesion is:

1) A possible crystalline orientation dependence for given faces in contact has been detected.
2) Indications of possible adhesion produced surface disruption have been obtained.
3) The adhesion between the silicates disappears in dry nitrogen.

Little needs to be said about the ionic-covalent forces. These are the normal bonding forces of the silicate lattice, as well as for the various metal oxides. They are highly directional and hence should show a significant crystalline orientation dependence; they are also, in general, the only forces of sufficient strength to produce surface disruption. These forces have the shortest range of effective action of all forces considered here, and hence their effectiveness is highly sensitive to the degree of surface contamination present. Evidence to date indicates that these forces contribute to the observed adhesion even though present surface cleaning techniques need considerable improvement.

2.4.3.5 Discussion of Results for Individual Sample Pairs

a. Orthoclase (001)/Orthoclase (001)

The data for these two runs are shown in Figure 11. The rapid increase in adhesion at higher loads is quite noticeable. The obvious question is what causes this? It can be stated first that if we were dealing with perfectly clean, and ideal, surfaces with distortion under load being due

only to simple elastic or plastic processes occurring at the contacting asperities, such a rapid increase could not be explained on any reasonable physical basis. However, we are not dealing with perfectly clean and ideal surfaces.

For the present case, there are two likely explanations for this rapid increase. First, the samples under load could move significantly closer together through lateral movement on a micro-scale resulting in a better mating (not wedging) of surface irregularities. Second, surface contamination is present. Under sufficiently high loading, penetration of this contamination could begin, allowing the ionic-covalent forces to come into play. It appears that both of these effects may be operative. As for the forces which are active in this range, it can only be stated at this time that the magnitude of the adhesion can be explained if ionic-covalent forces are acting; however, if the surfaces are brought into a much better mate under load, both mosaic charging and dispersion forces could account for the observations.

At higher loads, the slope of the curves begins to decrease, and a separation into two branches occurs. It appears that crystalline orientation effects are present and hence that the adhesion must be produced principally by ionic-covalent forces. However, any definitive conclusions in this regard are premature. First, the data are for two separate experimental runs with different samples (the samples, however, were cut from the same specimen). Second, variations in surface roughness as a function of direction could also produce a crystalline orientation effect, independent of the forces

acting. Roughness effects can be most troublesome if they are related to the crystal axes. The roughness plots of Figures 2 through 10 give no indication of this. However, the photomicrographs give the appearance of lineations parallel to the b-axis. Roughness profiles, at a much expanded horizontal scale, are being taken to determine whether these "lineations" represent an axis-oriented roughness. It should be noted, however, that care was taken in the orthoclase runs to ensure that the axes were not aligned, so that axis-oriented roughness effects would be minimized.

b. Orthoclase (001)/Hypersthene (110)

The appearance of these data, see Figure 11, are similar in many ways to those of the orthoclase/orthoclase runs, hence most of the same comments apply. The principal difference is the reduced magnitude of the adhesion. This would be expected if the ionic-covalent forces are acting.

This is the only sample pair run to date where minerals of significantly different color were contacted. As discussed previously, studies of the surfaces after contact showed hypersthene surface deposits on the orthoclase. It appears that this may have been produced by the vacuum adhesion. If so, then the ionic-covalent forces must have been acting.

c. Orthoclase (001)/Albite (001)

These data are shown in Figure 16. It is noted immediately that they have an entirely different character than the previous data: adhesion is present at zero load and it increases quite slowly with increasing load. This behavior was quite surprising in the light of the previous data. The only obvious physical difference (outside of crystalline structure) between

the albite and the other samples used is that the albite surface is much less rough. This leads to the suspicion that better mating of the surfaces under load, with the expected significant increase in true contact area, may be playing a major role in the initial rapid increase in the adhesion for the other samples tested. As for the nature of the forces acting, no definite discrimination between ionic-covalent, mosaic, and dispersion forces can be made, even though the load dependence aspect implies that the ionic-covalent forces may be acting. When time permits, this sample pair will be run again, to try again to see whether or not any evidence of the high adhesion noted on the previous runs can be obtained.

d. Orthoclase (001)/Pure Aluminum

These data are given in Figure 17. As discussed previously, it appears that the separation of the curve into two branches may be real. The lower branch is quite similar to the results obtained from the orthoclase/albite run; the upper branch bears some resemblance to the other silicate runs.

There are two possible physical reasons why two branches may exist. First, even though the metal sample was pure aluminum, the surface was aluminum oxide (no means are available in the vacuum system at the present time for the removal of metal oxides). This oxide layer overlays a soft, metallic substrate. For small load forces it may be that contact was solely between the orthclase and aluminum oxide, whereas at the higher loads penetration into the soft subsurface occurred. Large adhesions could be produced by this since the non-directional metallic bonds could become active, and because bulk plastic flow in the aluminum could occur, causing large increases in true contact area. The forces involved in this adhesion

(upper branch) would then most probably be the normal ionic-covalent and metallic bonding forces of the respective samples. The forces involved in the adhesion for the lower branch could, however, be any combination of the three types.

The second possible explanation does not require any penetration of the oxide layer. Instead, at the lower loads, adhesion could be primarily due to mosaic and/or dispersion forces with the ionic-covalent forces playing a minor, or no, role. However, as the load is increased, penetration of the surface contamination (excluding the oxide layer) is accomplished so that the ionic-covalent forces become predominant.

Preliminary study of the contacting surfaces has indicated the presence of aluminum on the orthoclase surface as well as some disruption of the aluminum surface. These observations indicate strongly that the ionic-covalent forces were active at some time during the run. The observations do not tell, however, whether or not penetration of the oxide layer occurred.

An interesting phenomenon occurred during this run. It was found that adhesion, of magnitude comparable to that of the lower branch of the vacuum curve, remained even after prolonged exposure to dry nitrogen. In addition, long range attractive forces were detected in nitrogen, but not in vacuum. The continued existence of adhesion in nitrogen implies that mosaic and/or dispersion forces were active. However, the observation that the adhesion decreased slowly with time, being rejuvenated only by applying a load, indicates the ionic-covalent forces may have been contributing. A final

decision on this point cannot be made at present, principally because the aluminum, being so soft, could be easily deformed with partial breakup of the oxide layer. It will be of considerable interest to see how these results compare with those obtained with metals of greater hardness, including aluminum alloys.

No good reason can presently be given as to why long range attractive forces were observed in nitrogen but not in air.

3.0 SUMMARY

Measurements of adhesion as a function of load have been made during this quarter. The sample pairs studied have been orthoclase (001)/orthoclase (001) (for two different orientations), orthoclase (001)/hypersthene (110), orthoclase (001)/albite (001), and orthoclase (001)/pure aluminum. A definite dependence of adhesion upon load force has been obtained. Adhesion forces in excess of 0.4 gm have been observed. The data indicate an adhesion dependence upon crystalline orientation.

With the exception of the orthclase/pure aluminum run, no evidence of long range forces has been obtained. It is concluded that, with the possible exception of the aluminum run, homogeneous surface charging does not play a significant role in the adhesion. Study of the contacting surfaces with the petrographic microscope indicates material transfer has occurred. This transfer may be a direct result of the adhesion, in which case the ionic-covalent bonding forces must have been active. The largest values obtained for the adhesion can be explained on the basis of ionic-covalent forces;

also by mosaic and/or dispersion forces if, and only if, under load the contacting surfaces move much closer together (into better mate). Indications as to crystalline orientation dependence, the vanishing of adhesion in dry nitrogen, the lack of any significant effect of prior loading on zero load adhesion, and the fact that the largest adhesions were detected for the surfaces of greatest similarity, atomically speaking, provide additional evidence for the major role played by the ionic-covalent forces.

The obtaining of additional detailed data on these and other materials will aid greatly in resolving the present uncertainties.